GLIA

GLIA 60:1555–1566 (2012)

Oligodendroglia are Limited in Type I Interferon Induction and Responsiveness *In Vivo*

PARUL KAPIL,[1,2] NIRANJAN B. BUTCHI,[1] STEPHEN A. STOHLMAN,[1] AND CORNELIA C. BERGMANN[1]*
[1]*Department of Neurosciences, NC-30, Lerner Research Institute, Cleveland Clinic Foundation, Cleveland, Ohio*
[2]*Department of Biological, Geological, and Environmental Sciences, Cleveland State University, Cleveland, Ohio*

KEY WORDS
coronavirus; central nervous system; innate immunity; IFNα/β; oligodendroglia

ABSTRACT
Type I interferons (IFNα/β) provide a primary defense against infection. Nevertheless, the dynamics of IFNα/β induction and responsiveness by central nervous system (CNS) resident cells *in vivo* in response to viral infections are poorly understood. Mice were infected with a neurotropic coronavirus with tropism for oligodendroglia and microglia to probe innate antiviral responses during acute encephalomyelitis. Expression of genes associated with the IFNα/β pathways was monitored in microglia and oligodendroglia purified from naïve and infected mice by fluorescent activated cell sorting. Compared with microglia, oligodendroglia were characterized by low basal expression of mRNA encoding viral RNA sensing pattern recognition receptors (PRRs), IFNα/β receptor chains, interferon sensitive genes (ISG), as well as kinases and transcription factors critical in IFNα/β signaling. Although PRRs and ISGs were upregulated by infection in both cell types, the repertoire and absolute mRNA levels were more limited in oligodendroglia. Furthermore, although oligodendroglia harbored higher levels of viral RNA compared with microglia, *Ifn*α/β was only induced in microglia. Stimulation with the double stranded RNA analogue poly I:C also failed to induce *Ifn*α/β in oligodendroglia, and resulted in reduced and delayed induction of ISGs compared with microglia. The limited antiviral response by oligodendroglia was associated with a high threshold for upregulation of *Ikk*ε and *Irf7* transcripts, both central to amplifying IFNα/β responses. Overall, these data reveal that oligodendroglia from the adult CNS are poor sensors of viral infection and suggest they require exogenous IFNα/β to establish an antiviral state.

INTRODUCTION

Type I interferons (IFNα/β) are critical innate cytokines that limit viral replication and dissemination prior to the emergence of adaptive immune responses. In addition to inducing an antiviral state, IFNα/β exert numerous other functions including induction of apoptosis, mobilizing innate cells, and regulating adaptive immune responses (Barton, 2008; Borden et al., 2007; Stetson and Medzhitov, 2006; Vilcek, 2006). As these pleiotropic effects can be detrimental if left unregulated, the innate antiviral response has to be controlled to minimize cell injury and maintain cellular homeostatic functions. Although an early IFNα/β response contributes to viral control and disease outcome, its precise regulation is especially critical in the central nervous system (CNS), where the health of nonrenewable neurons as well as resident glia is vital for the maintenance of host physiological function. IFNα/β production and signaling is thus tightly regulated by both the basal and inducible expression of numerous factors involved in the IFNα/β pathway.

During viral infections the ability to induce IFNα/β is determined by activation of pattern recognition receptors (PRR) following interaction with pathogen associated molecular patterns, which typically constitute viral RNA or DNA structures. PRRs comprise members of the Toll-like receptor (TLR) family and the cytosolic helicase sensors, retinoic acid-inducible gene 1 (RIG-I), and melanoma differentiation-associated antigen 5 (MDA5) (Kawai and Akira, 2009; Mogensen, 2009). PRR recognition of viral RNA triggers the activation and nuclear localization of interferon regulatory factors (IRF) IRF3 and IRF7 leading to IFNα/β induction. By binding to its receptor, secreted IFNα/β initiates a signaling cascade leading to transcription of a variety of interferon stimulated genes (ISG). ISG encode both direct antiviral factors as well as PRR and signal transduction components, such as IRF7 and STAT1 (Borden et al., 2007). This amplification loop thus elevates the ability of cells to induce and respond to IFNα/β. In general IRF7 is considered the master switch in IFNα/β induction following various viral infections due to its role in amplifying IFNα/β production (Honda and Taniguchi, 2006). Because the pattern as well as levels of PRR, IRF, and IFNα/β receptor expression and activation varies with each cell type, initial IFNα/β induction and amplification can be very distinct depending on the cell types infected (Colonna, 2007; Stewart et al., 2005). Furthermore, due to the potency of IFNα/β in inhibiting viral replication, many viruses have evolved mechanisms to antagonize the IFNα/β pathway, either at the induction or signaling

Additional Supporting Information may be found in the online version of this article.

Grant sponsor: National Institute of Health; Grant number: P01 NS064932.

*Correspondence to: Cornelia C. Bergmann, Lerner Research Institute, Cleveland Clinic Foundation, 9500 Euclid Avenue, Cleveland, OH 44195.
E-mail: bergmac@ccf.org

Received 11 January 2012; Accepted 31 May 2012

DOI 10.1002/glia.22375

Published online 26 June 2012 in Wiley Online Library (wileyonlinelibrary.com).

level (Levy and Garcia-Sastre, 2001; Sen, 2001). Microglia and astrocytes are primary sentinels within the CNS parenchyma responding to stimuli triggered by either microbial infection or degenerative events (Dong and Benveniste, 2001; Hanisch, 2002; Paul et al., 2007). This function is partially attributed to basal expression of a vast array of PRRs (Bsibsi et al., 2002; Carty and Bowie, 2011; Hanke and Kielian, 2011; Okun et al., 2009; van Noort and Bsibsi, 2009). *Irf3* mRNA, and to a lesser extent *Irf7* mRNA, are constitutively expressed in the CNS. While *Irf7* expression is highly inducible, *Irf3* transcripts remain constant following infection (Ousman et al., 2005). However, their relative expression in different cell types has not been extensively explored. Consistent with PRR activation, microglia, astrocytes, and neurons all induce IFNα/β (Paul et al., 2007). However, the vast majority of information on CNS innate responsiveness is derived from primary glia and neuronal cultures established from neonates and may not reflect responsiveness of fully differentiated cells. Distinct from *in vitro* studies, IFNα/β production *in vivo* is highly restricted as indicated by the small proportion (<5%) of infected neurons with detectable IFNα/β expression in mice infected with lymphocytic choriomeningitis virus (Delhaye et al., 2006). Furthermore, IFNα/β inducible *Irf7* transcripts mapped closely to sites of viral RNA (Ousman et al., 2005), supporting highly focal IFNα/β responses. Overall however, little is known about responsiveness of distinct CNS cell types to viral infections *in vivo*. Specifically oligodendroglia appear to express a limited TLR repertoire at basal levels compared with microglia (Hanke and Kielian, 2011; Okun et al., 2009; Paul et al., 2007). They also do not appear to contribute to extensive proinflammatory cytokine secretion (Cannella and Raine, 2004).

Infection with the neurotropic mouse hepatitis virus (MHV) strain JHM (JHMV), belonging to the positive strand RNA coronavirus family, was used to better characterize the ability of oligodendroglia to mount innate antiviral immune responses *in vivo* based on its prominent infection and persistence in oligodendroglia (Bergmann et al., 2006). In adult mice, JHMV infection causes an acute encephalomyelitis, which resolves into a persistent infection of the spinal cord associated with demyelination. In addition to oligodendroglia, JHMV also infects microglia and infiltrating macrophages during acute infection; however, neuronal and astrocyte infection is sparse (Ireland et al., 2008, 2009). Coronaviruses are poor inducers of IFNα/β in numerous cell types due to their 5′RNA structures mimicking self RNA (Daffis et al., 2010; Zust et al., 2011). However, IFNα/β is induced in microglia, macrophages, and plasmacytoid dendritic cells (Cervantes-Barragan et al., 2007; Roth-Cross et al., 2008). Importantly, a protective effect of IFNα/β *in vivo* was highlighted by uncontrolled MHV replication in mice deficient in IFNα/β signaling (Cervantes-Barragan et al., 2007; Ireland et al., 2008). Furthermore, protection following peripheral MHV infection is associated with TLR7 dependent IFNα/β production by plasmacytoid dendritic cells (Cervantes-Barragan et al., 2007). The naïve CNS is devoid of plasmacytoid dendritic cells (Serafini et al., 2000), implicating infected glia as primary candidates contributing to protective IFNα/β production following CNS infection. This is supported by MDA5 mediated IFNα/β production in infected microglia (Roth-Cross et al., 2008).

In the present study we compared the relative IFNα/β responsiveness of oligodendroglia and microglia following infection with JHMV or intracerebral inoculation of the double stranded RNA mimic poly I:C. Both glia populations were isolated directly from the CNS to monitor changes in mRNA expression. These results are the first to imply an inherent paucity in IFNα/β transcription by oligodendroglia, coincident with limited expression of PRR and signaling molecules downstream of PRR activation. The dependence of oligodendroglia on IFNα/β from other cellular sources to induce an antiviral state *in vivo* highlight the potent monitoring functions of microglia and suggest a mechanism to preserve oligodendroglial homeostatic functions.

MATERIALS AND METHODS

Mice, Virus, and Poly I:C Injection

C57BL/6 wild type (Wt) mice were purchased from the National Cancer Institute (Frederick, MD). Mice expressing green fluorescent protein (GFP) under the control of the proteolipid protein (PLP) promoter (PLP-GFP) (Fuss et al., 2000) were backcrossed six times with C57BL/6 mice prior to use (Malone et al., 2008). Congenic mice defective in IFNα/β signaling ($IFNAR^{-/-}$) were previously described (Ireland et al., 2008). Mice at 6–7 weeks of age were infected via intracerebral injection with 250 Plaque Forming Units of the neutralizing monoclonal antibody (mAb)-derived JHMV variant, designated V2.2v-1 (Fleming et al., 1986) in 30 μL of endotoxin-free Dulbecco's modified phosphate-buffered saline (PBS). In some experiments, the double stranded RNA mimic poly I:C (Invitrogen, Carlsbad, CA; high molecular weight) was injected intracerebrally into 6- to 7-week-old C57BL/6 mice at a concentration of 200 μg in 30 μL endotoxin-free PBS. All mice were housed and bred under pathogen-free conditions at an accredited facility at the Lerner Research Institute, Cleveland Clinic. All procedures were in compliance with animal protocols approved by the Institutional Animal Care and Use Committee.

CNS Cell Isolation by Fluorescent Activated Cell Sorting (FACS) and *Ex Vivo* Poly I:C Treatment

Mononuclear cells were isolated from spinal cords as described previously (Malone et al., 2008; Phares et al., 2009). Briefly, spinal cords from six to seven mice were finely minced, digested in PBS containing 0.25% trypsin for 30 min at 37°C, and trypsin quenched by addition of 20% new born calf serum. Following centrifugation at 400*g* for 7 min, cells were resuspended in 30% Percoll (Pharmacia, Uppsala, Sweden) and concentrated by cen-

trifugation for 30 min at 800*g* at 4°C onto a 1 mL 70% Percoll cushion. Cells collected from the 30%/70% Percoll interface were washed with RPMI medium containing 25 mM HEPES (pH 7.2), viable cells determined by trypan blue exclusion, and incubated in PBS supplemented with 5% Bovine Serum Albumin (BSA) (1× FACS buffer), 1% mouse serum and anti-mouse CD16/32 (clone 2.4G2; BD Pharmingen, San Diego, CA) for 15 min at 4°C to block nonspecific antibody binding. Cell populations were identified by four-color staining with phycoerythrin (PE)-, fluorescein isothiocyanate-, peridinin chlorophyll protein-, or allophycocyanin-conjugated mAb. CNS infiltrating macrophages and resident microglia were distinguished by staining with anti-CD45 (30-F11), and anti-F4/80 mAb (Serotec, Raleigh, NJ). Infiltrating macrophages were characterized by their $CD45^{hi}$ $F4/80^{+}$ and microglia by their $CD45^{low}$ $F4/80^{+}$ phenotype, respectively. PLP-GFP transgenic mice facilitated identification of oligodendroglia via their $CD45^{-}$ GFP^{+} phenotype (Malone et al., 2008). Oligodendroglia from $IFNAR^{-/-}$ and Wt control mice were identified by consecutive staining with unconjugated O4 mAb and anti-mouse IgM (PE) mAb (R6-60.2) (BD Pharmingen) and purified based on their $CD45^{-}$ $O4^{+}$ phenotype as described (Gonzalez et al., 2005; Phares et al., 2011). Cells were purified on a BD FACSAria (BD Biosciences), resuspended in TRIzol (Invitrogen, Carlsbad, CA) and stored at −80°C. Typical yields for six to seven naïve spinal cords were $4–8 \times 10^4$ oligodendroglia and $4–6 \times 10^5$ microglia. For *ex vivo* poly I:C stimulation, FACS sorted microglia and oligodendroglia were incubated with 10 μg mL^{-1} poly I:C alone or together with the FuGENE 6 transfection reagent (Roche diagnostics, Indianapolis, IN) in DMEM for 8 h following the manufacturer's protocol. Fetal calf serum was added to a final concentration of 5% after 1 h.

Quantitative Real-time PCR

RNA was extracted by dissociation in TRIzol reagent (Invitrogen) according to the manufacturer's instructions and subjected to real-time PCR analysis as described (Phares et al., 2011). In brief, snap-frozen spinal cords or FACS-purified cells were homogenized with TRIzol in a Tissuelyser II (Qiagen, Valencia, CA) or by pipetting, respectively, and treated with chloroform. RNA was precipitated with isopropyl alcohol, washed with 75% ethanol, and resuspended in RNase-free water (Gibco/Invitrogen, Grand Island, NY). Following DNAse treatment using a DNA Free™ kit (Ambion, Austin, TX) cDNA was synthesized using Moloney murine leukemia virus reverse transcriptase (Invitrogen) in buffer containing 10 mM deoxynucleoside triphosphate mix, 250 ng random hexamer primers and oligo(dT) (1:1 ratio) (Invitrogen). Quantitative real-time PCR was performed for mRNA expression levels of IFNAR receptor chains, IKKε, virus-nucleocapsid (N) protein, MDA5, RIG-I and IFNλ using SYBR green master mix (Applied Biosystems, Foster city, CA). The primer sequences are as follows (F, forward; R, reverse): IFNAR1, F,5′-CCCAAGGCAAGAGCTATGTC-3′, and R,5′-TCTGAACGGCTTCCAGAACT-3′; IFNAR2a (soluble), F,5′-GATGATGACCCCGCAATAAA-3′, and R,5′-AAAACAATAGTGCAAATTTTAAAAACC-3′; IFNAR2c (transmembrane), F,5′-GGCAGTGACAGTGACGAAGA-3′, and R,5′-CTGGCTGAGGTGTCAGAGGT-3′; IKKε, F,5′-CCAGAAGATTCAGTGTTGTTTGG-3′, and R,5′-TCATTGTAGCTGAGCCCTG-3′; JHMV-N, F,5′-CGCAGAGTATGGCGACGAT-3′, and R,5′-GAGGTCC TAGTCTCGGCCTGTT-3′; MDA5, F,5′-GACACCAGAATT CAAGGGAC-3′, and R,5′-GCCACACTTGCAGA TAATCTC-3′; RIG-I, F,5′-GTCAGCACAAACCACAACC-3′, and R,5′-GTCTCAACCACTCGAATGTC-3′; IFNλ, F,5′-AGCTGCAGGCCTTCAAAAAG-3′, and R,5′-TGGGAGTGAATGTGGCTCAG-3′. Reactions were monitored using the 7500 Fast Real Time PCR system (Applied Biosystems) under the following conditions: 95°C for 10 min, followed by 40 cycles of denaturation at 94°C for 10 s, annealing at 60°C for 30 s, and elongation at 72°C for 30 s. Expression levels of *Adar1*, *Gapdh, Ifna4, Ifn*β*, Ifit1, Ifit2, Irf3, Irf7, Irf9, Stat1, Tlr3*, and *Tlr7* were determined by using TaqMan primer and probe sets, and 2× universal TaqMan fast master mix (Applied Biosystems). TaqMan PCR reactions were performed in 10 μL final reaction volumes containing specific master mix, 1 mM concentrations of each primer mix, and 4 μL of cDNA using the ABI 7500 fast PCR and 7500 software. All TaqMan reactions were initiated by incubation at 95°C for 20 s, followed by 40 cycles of denaturation at 95°C for 30 s and annealing and extension at 60°C for 30 s. Transcript levels for both SYBR and Taqman assays were calculated relative to the housekeeping gene glyceraldehyde-3-phosphate dehydrogenase (GAPDH) using the following formula: $2^{[CT(GAPDH) - CT(Target\ Gene)]} \times 1{,}000$, where CT represents the threshold cycle at which the fluorescent signal becomes higher than the background (Kapil et al., 2009; Phares et al., 2009).

The CNS cell isolation procedure routinely yielded higher numbers of microglia compared with oligodendroglia. To validate that RNA isolation from a low cell number was not a factor limiting detection of low abundance mRNA, minimum cell numbers needed to achieve reliable PCR products were determined. For this purpose brain-derived $CD45^{lo}$ $CD11b^{+}$ microglia were purified by FACS from mice injected with poly I:C 4 h prior to isolation. RNA was separately isolated from increasing cell numbers starting with as few as 7,500 up to 240,000 cells and analyzed for *Gapdh, Ifna4*, *Ifn*β, *Ifit1*, and *Ifit2* transcripts. Titration curves demonstrate that Ct values were in the linear range down to 30,000 cells, even for low copy number *Ifna4* transcripts (Supp. Info. Fig. 1). A minimum of 30,000–40,000 cells were thus used for real time PCR analysis.

RESULTS

Limited Expression of PRR and Signal Transduction Molecules in Oligodendroglia

Induction of IFNα/β by murine coronaviruses is mediated via TLR7 in pDC and via MDA5 in microglia/mono-

cytes (Cervantes-Barragan et al., 2007; Roth-Cross et al., 2008). Furthermore, both MDA5 and RIG-1 act as PRR in an oligodendroglia cell line (Li et al., 2010). However, the expression of these viral sensors in oligodendroglia in the adult CNS is unknown. To analyze their capacity to initiate innate responses, oligodendroglia and microglia were isolated from spinal cords of uninfected PLP-GFP mice by FACS based on their respective $CD45^{-}$ GFP^{+} and $CD45^{lo/int}$ $F4/80^{+}$ phenotypes (Malone et al., 2008). Spinal cords were used as donor tissue based on higher oligodendroglia yields compared with brains. The potential of mature oligodendroglia to recognize viral RNA in comparison to microglia was assessed by comparing basal transcript levels of genes encoding the viral RNA sensors MDA5, RIG-I, TLR3, and TLR7 (Kawai and Akira, 2007). Whereas transcription of all four PRR was readily detected in microglia, *Mda5*, *Rig-I*, and *Tlr3* transcripts were significantly reduced and *Tlr7* was below detection in oligodendroglia (Fig. 1A). Basal levels of PRR mRNAs are low in the resting CNS relative to lymphoid tissue, with the exception of *Tlr3* (McKimmie et al., 2005). Nevertheless, PRR are rapidly upregulated during viral encephalitis initiated by Semliki Forest virus, Rabies virus, and Venezuelan Equine Encephalitis virus (McKimmie et al., 2005; Sharma and Maheshwari, 2009). However, the relative contribution of infiltrating leukocytes versus resident CNS cells was not directly assessed. Microglia and oligodendroglia were therefore isolated from JHMV infected mice to evaluate upregulation of PRRs during the course of infection. Microglia upregulated *Mda5*, *Rig-I*, *Tlr3*, and *Tlr7* transcripts two- to fivefold over basal levels, with peak expression at Days 3–5 postinfection (p.i.) (Fig. 1B). Relative to the modest fold increase in microglia, *Mda5* and *Rig-I* transcripts were vastly increased in oligodendroglia. *Rig-I* expression reached levels similar to microglia by Day 3 p.i. amounting to an ~70 fold increase over naïve levels (Fig. 1). Nevertheless, *Mda5* mRNA levels in oligodendroglia remained overall lower compared with microglia. Similarly, mRNAs encoding the endosomal PRR TLR3 and TLR7 were also induced in oligodendroglia, but absolute levels remained low and peak expression was delayed relative to microglia. Induction of *Mda5* and *Rig-I* in oligodendroglia, as well as all RNA sensing PRR in microglia, correlated with induction of *Ifnα4* and *Ifnβ* mRNA in the CNS following JHMV infection (Ireland et al., 2008; Malone et al., 2008). To evaluate additional contributions of Type II (IFNγ) and Type III (IFNλ) IFN, which also induce ISG, the RNA expression kinetics of all three IFN families were assessed in spinal cords (Fig. 2). Confirming previous results (Malone et al., 2008) *Ifnα4* and *Ifnβ* mRNA were increased at Day 3 and peaked at Day 5 p.i. Although there are three Type III IFNλ family members, IFNλ1 is a pseudogene in mice; therefore primers were used to detect IFNλ2/3. IFNλ was minimally induced, yet with similar kinetics as IFNα/β, confirming very low expression and function in the CNS following heterologous infections, including a closely related MHV strain (Sommereyns et al., 2008). IFNγ mRNA was not upregulated until Day 5 p.i., and increased substantially by Day 7 p.i. As both IFNα/β and IFNγ signaling target many overlapping ISG, a contribution of early IFNγ to increased PRR expression could thus not be excluded.

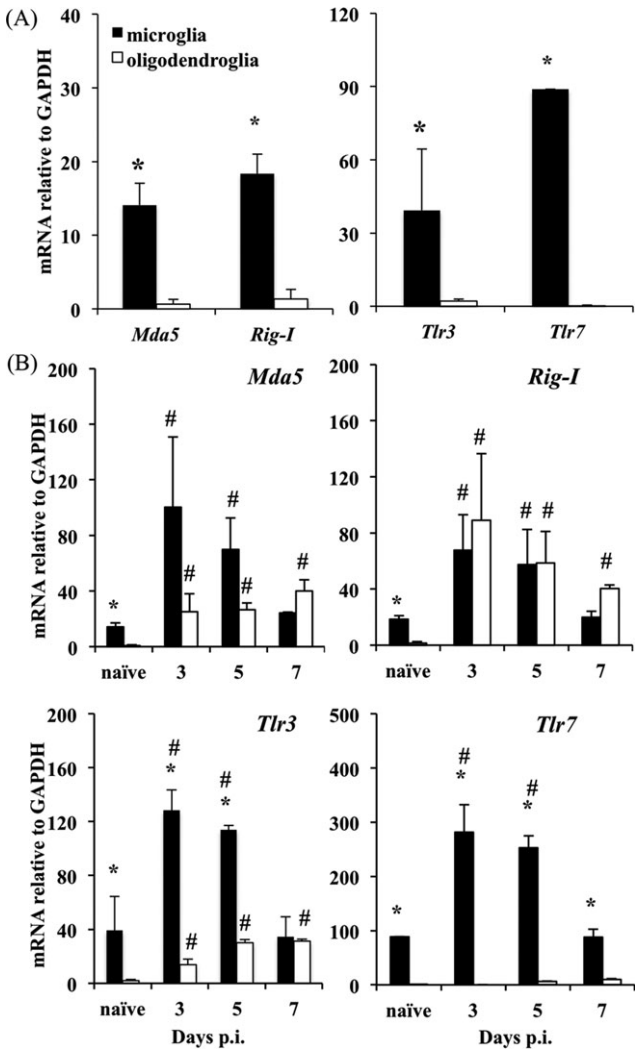

Fig. 1. Oligodendroglia are limited in basal and inducible expression of viral RNA sensing PRRs. Microglia and oligodendroglia purified from spinal cords of naïve (**A**) or JHMV infected (**B**) PLP-GFP mice were assayed for *Mda5*, *Rig-I*, *Tlr3*, and *Tlr7* transcripts at the indicated times p.i. Data represent the average of three separate experiments ± standard error of the mean (SEM). "*" denotes $P \leq 0.05$ comparing microglia to oligodendroglia at each timepoint; "#" indicates $P \leq 0.05$ compared with basal levels for each cell population.

To verify that the increase in PRR transcripts is directly attributed to IFNα/β signaling, mRNA expression was assessed in microglia and oligodendroglia from naïve and JHMV infected Wt and $IFNAR^{-/-}$ mice. Although basal *Mda5* and *Rig-I* mRNA levels were diminished by eight- to ninefold in microglia from naïve $IFNAR^{-/-}$ relative to Wt mice, they were only slightly reduced in oligodendroglia (Fig. 3). These results are reminiscent of previous observations that PRR expression in neurons is controlled by basal IFNα/β signaling (Shrestha et al., 2003). Importantly, the absence of IFNα/β signaling abrogated upregulation of *Mda5* and

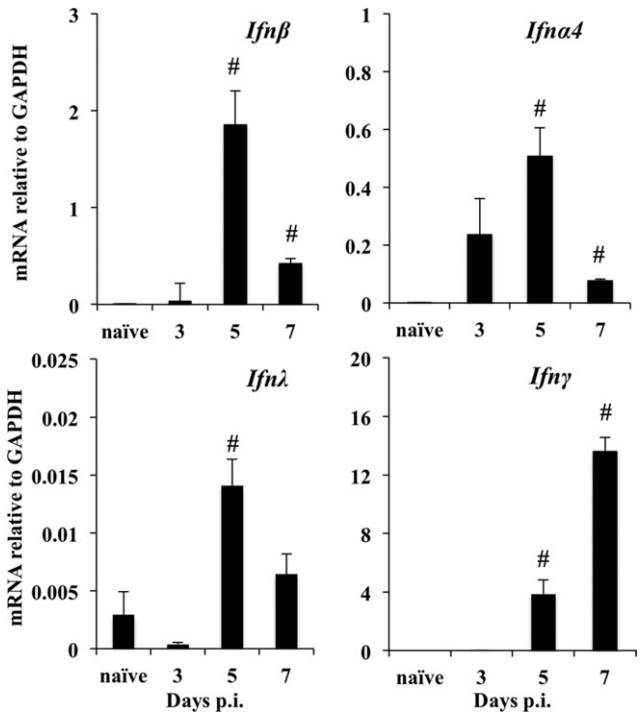

Fig. 2. Kinetics of IFNα/β, IFNλ, and IFNγ expression during viral infection. Wt mice infected with JHMV were analyzed for kinetics of *Ifn*β, *Ifnα4*, *IFN*λ, and *IFN*γ mRNA induction in spinal cords. Data represent the mean ± SEM for three mice per group; "#" indicates $P \leq 0.05$ compared with basal levels.

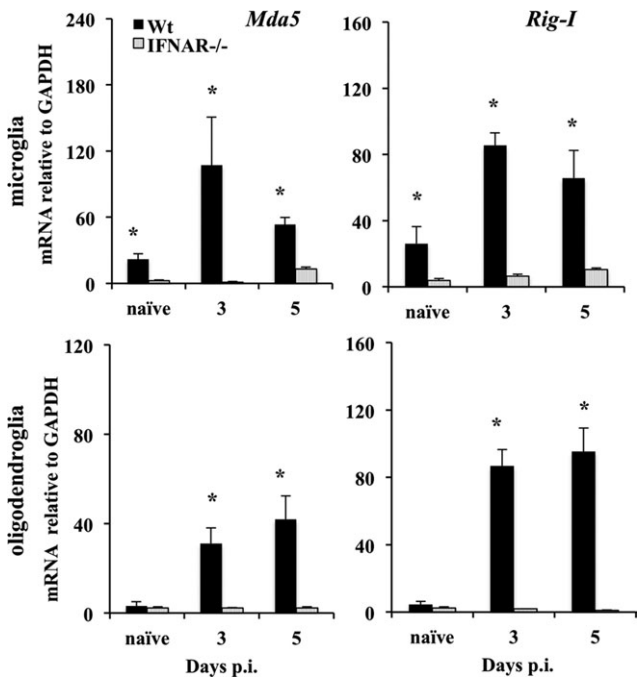

Fig. 3. MDA5 and RIG-I upregulation is IFNα/β dependent. Wt and IFNAR$^{-/-}$ mice infected with JHMV were used to compare induction of *Mda5* and *Rig-I* mRNA in oligodendroglia and microglia purified from spinal cords. Data are average of three individual experiments ± SEM as described in Fig. 1. "*" denotes $P \leq 0.05$ comparing wt to IFNAR$^{-/-}$ populations at each timepoint.

Rig-I transcripts in both microglia and oligodendroglia following JHMV infection (Fig. 3). Early induction of *Mda5* and *Rig-I*, both classified as ISG, thus demonstrated that oligodendroglia respond to exogenous IFNα/β *in vivo*, similar to microglia. IFNα/β thus enhances the potential to recognize invading RNA viruses, thereby facilitating early innate responses.

IFNα/β is not Induced in Oligodendroglia

IFNα/β signaling is crucial to prevent dissemination of gliatropic coronavirus within the CNS parenchyma (Ireland et al., 2008). Furthermore, IFNα/β induction in response to coronavirus infection has been demonstrated in microglia *in vitro* and *in vivo* (Roth-Cross et al., 2008) as well as in an oligodendroglial cell line (Li et al., 2010). Given the distinct basal and inducible levels of *Mda5* transcripts in mature CNS derived glial populations, the contribution of infected oligodendroglia and microglia to IFNα/β induction was assessed *in vivo* by comparing *Ifn*β and *Ifnα4* mRNA relative to viral replication in each population. Viral loads were monitored by measuring viral mRNA encoding the N protein, the most abundant viral RNA in infected cells (Skinner and Siddell, 1983). Viral-N transcripts prevailed in microglia at Day 3 p.i., but decreased by Days 5 and 7 p.i. (Fig. 4). By contrast, although viral mRNA was near detection levels at Day 3 p.i. in oligodendroglia, the levels increased ~20 fold relative to microglia by Day 5 p.i. Despite subsiding by Day 7 p.i., viral mRNA levels remained significantly elevated relative to microglia. These results not only assured that infected cells were recovered by the isolation procedure, but clearly indicated that virus predominated in microglia early, but subsequently prevailed in oligodendroglia. Concomitant with infection, sparse but detectable basal levels of *Ifn*β and *Ifna4* transcripts increased in microglia (Fig. 4). *Ifn*β levels were sustained through Day 5 p.i., while *Ifnα4* levels were only transiently upregulated. The contribution of infiltrating infected monocyte-derived macrophages (Ireland et al., 2009) to *Ifn*α/β induction was also assessed. Viral RNA loads in macrophages were <50% of those in microglia and declined with similar kinetics; *Ifn*α/β transcripts reflected the magnitude of viral RNA transcripts similar to microglia (data not shown). By contrast, neither *Ifnα4* nor *Ifn*β mRNA were detected in oligodendroglia from naïve or infected mice (Fig. 4), despite higher viral RNA loads as well as elevated *Mda5* and *Rig-I* mRNA by Day 5 p.i. (Fig. 3).

The failure of oligodendroglia to induce *Ifn*α/β following infection suggested that MDA5 and RIG-I are not activated, and/or that downstream signaling factors are limiting. PRR signaling requires several mediators including the inducible kinase IKKε (also known as Ikbke or Ikki) and the transcription factors IRF3 and IRF7. While IRF3 is constitutively expressed, IRF7 is induced by IFNα/β and amplifies IFNα/β production (Honda and Taniguchi, 2006; Honda et al., 2005). There-

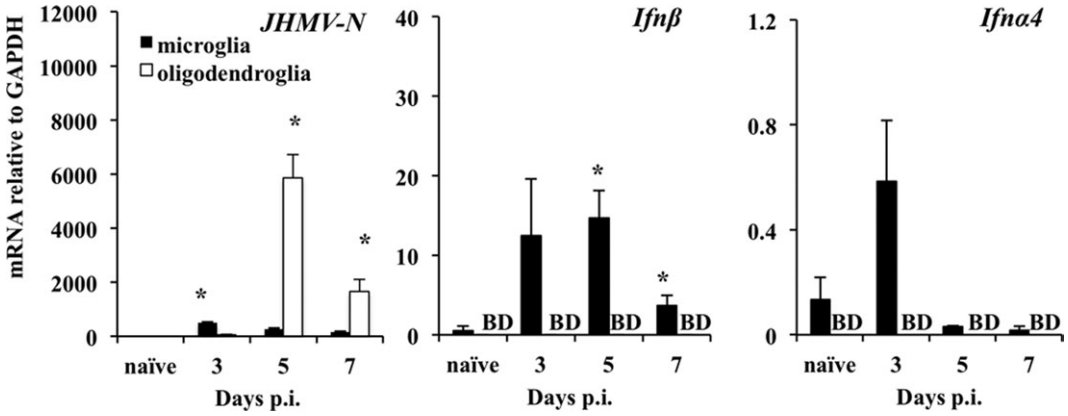

Fig. 4. Oligodendroglia do not induce IFNα/β transcripts during JHMV infection. Microglia and oligodendroglia purified from spinal cords of naïve or JHMV infected PLP-GFP mice were assessed for *JHMV-N*, *Ifn*β, and *Ifnα4* transcripts. Data are average values ± SEM of three independent experiments. BD indicates below detection. "*" denotes $P \leq 0.05$ comparing microglia to oligodendroglia.

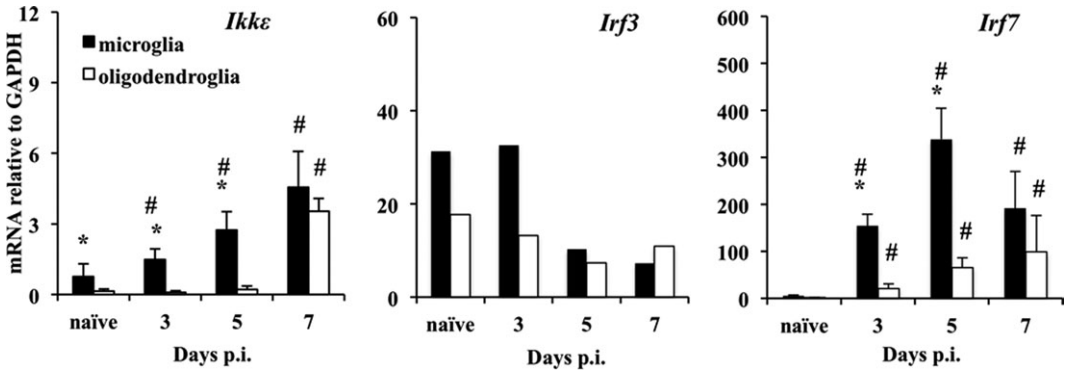

Fig. 5. Oligodendroglia are limited in basal and inducible expression of PRR associated signaling factors during JHMV infection. Microglia and oligodendroglia from naïve or JHMV-infected mice were assayed for *Ikk*ε, *Irf3*, and *Irf7* transcripts as indicated in Fig. 1. Data show the average of three separate experiments ± SEM for *Ikk*ε and *Irf7* and represent one of three separate experiments with similar results for *Irf3*. "*" denotes $P \leq 0.05$ comparing microglia to oligodendroglia at each timepoint; "#" indicates $P \leq 0.05$ compared with basal levels for each cell population.

fore to investigate the potential for PRR signaling, oligodendroglia were examined for expression of mRNAs encoding IKKε, IRF3, and IRF7. All three mRNAs were regulated in a cell type-specific manner (Fig. 5). Microglia from naïve mice expressed higher basal *Ikk*ε transcripts compared with oligodendroglia, which were modestly, but progressively upregulated throughout Day 7 p.i. (Fig. 5). By contrast, *Ikk*ε induction was not detected in oligodendroglia until Day 7 p.i., at which time levels reached those in microglia. *Irf3* mRNA was readily detected at basal levels in both microglia and oligodendroglia from naïve mice, but tended to decline following infection (Fig. 5). Lastly, *Irf7* transcripts were sparse in both microglia and oligodendroglia derived from naive mice (Fig. 5), consistent with lower basal CNS expression relative to *Irf3* (Ousman et al., 2005). However, in contrast to the increase of *Irf7* mRNA detected in microglia by Day 3 p.i., induction was more modest and occurred delayed in oligodendroglia following infection (Fig. 5). As the *Irf7* gene is an ISG, its upregulation in microglia was consistent with IFNα/β upregulation. By contrast, the delayed response in oligodendroglia implied more selective ISG induction and/or distinct IFNα/β receptor signaling thresholds.

Oligodendroglia Induce ISG Delayed Relative to Microglia

Upregulation of the ISGs *Rig-I*, *Mda5*, *Tlr3*, and *Irf7* support the notion that oligodendroglia respond to IFNα/β following infection. However, optimal induction was delayed and absolute levels were not as robust as in microglia. These results suggested that oligodendroglia is exposed to limiting amounts of IFNα/β in the microenvironment, or that they are intrinsically more limited than microglia in IFNα/β responsiveness. While the first possibility is difficult to address *in vivo*, the second may reflect reduced expression of the IFNα/β receptor (IFNAR) or downstream signaling components. We therefore assessed regulation of transcripts encoding the IFNAR, as well as STAT1 and IRF9, which act down-

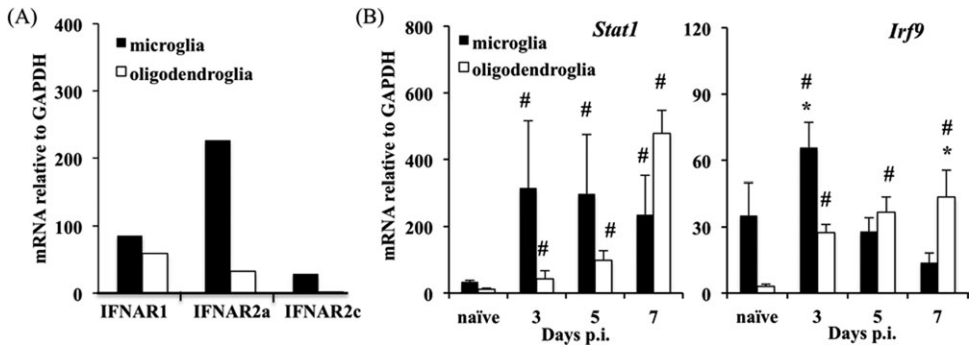

Fig. 6. Oligodendroglia have limited IFNα/β receptor signaling capacity. Microglia and oligodendroglia from naïve or JHMV infected mice were assayed for transcripts encoding the IFNAR1, soluble IFNAR2 (IFNAR2a) and IFNAR2 transmembrane (IFNAR2c) chains (**A**) or *Stat1* and *Irf9* transcripts (**B**). Data in (A) represent the average of two experiments; data in (B) represent the average of three independent experiments ± SEM as indicated in Fig. 1. "*" denotes $P \leq 0.05$ comparing microglia to oligodendroglia at each timepoint; "#" indicates $P \leq 0.05$ compared with basal levels for each cell population.

stream of IFNα/β signaling. IFNα/β binds a common receptor complex consisting of two transmembrane proteins, IFNAR1 and IFNAR2. As IFNAR2 exists as a soluble (IFNAR2a) and transmembrane (IFNAR2c) and isoform generated by alternative splicing (Domanski et al., 1995), we examined basal expression patterns of IFNAR1, and both IFNAR2 isoforms in microglia and oligodendroglia. Basal mRNA levels of the *Ifnar1* chain were approximately twofold higher in microglia compared with oligodendroglia. However, transcripts encoding both the soluble as well as the transmembrane form of *Ifnar2* were more than fivefold higher in microglia compared with oligodendroglia (Fig. 6A), suggesting more limited responsiveness of oligodendroglia to IFNα/β. *Stat1* and *Irf9* levels were also elevated in microglia compared with oligodendroglia derived from naïve mice (Fig. 6B). STAT1 is inducible by both IFNα/β and IFNγ, while IRF9 is constitutively expressed in most non CNS cell types (Borden et al., 2007). Consistent with a response to IFNα/β, *Stat1* mRNA indeed increased ~10 fold by Day 3 p.i. and remained elevated until Day 7 p.i. in microglia (Fig. 6B). By contrast, a reduced capacity of oligodendroglia to respond to IFNα/β was supported by the modest upregulation of *Stat1* transcripts at Days 3 and 5 p.i. The prominent increase of *Stat1* at Day 7 p.i. suggested IFNγ mediated upregulation. *Irf9* transcripts were only upregulated twofold in microglia by Day 3 p.i. and subsequently declined to or below basal levels (Fig. 6B). Nevertheless, despite lower basal levels and apparent constitutive expression, *Irf9* transcripts in oligodendroglia rapidly increased by ~15 fold at Day 3 p.i. and remained stable to Day 7 p.i. Although activation and nuclear localization of STAT1 and IRF9 remains to be evaluated, the overall limited basal levels of *Ifnar1* and *Ifnar2*, as well as basal and inducible levels of *Stat1* and *Irf9* transcripts in oligodendroglia during JHMV infection, support an inherent paucity in ISG transcriptional activation.

The notion of limited ISG transcriptional activation in oligodendroglia was further supported by analysis of a subset of ISG encoding factors with antiviral activity. Basal levels of transcripts encoding protein kinase R (*Pkr*), and the OAS/RNaseL pathway (*Oas2*), known to modulate translational activity, were all elevated in microglia derived from naïve mice relative to oligodendroglia (Fig. 7). Transcripts encoding adenosine deaminase specific for mRNA (Adar1), which limits viral replication via introduction of mRNA mutations (Bass, 1997), were also more abundant in microglia (Fig. 7). By contrast, *Ifit2* RNA was expressed at similar levels in both cell types derived from naïve mice. Importantly, in microglia all transcripts, particularly *Oas2* and *Ifit2* RNA, were rapidly increased to peak levels by Day 3 p.i.

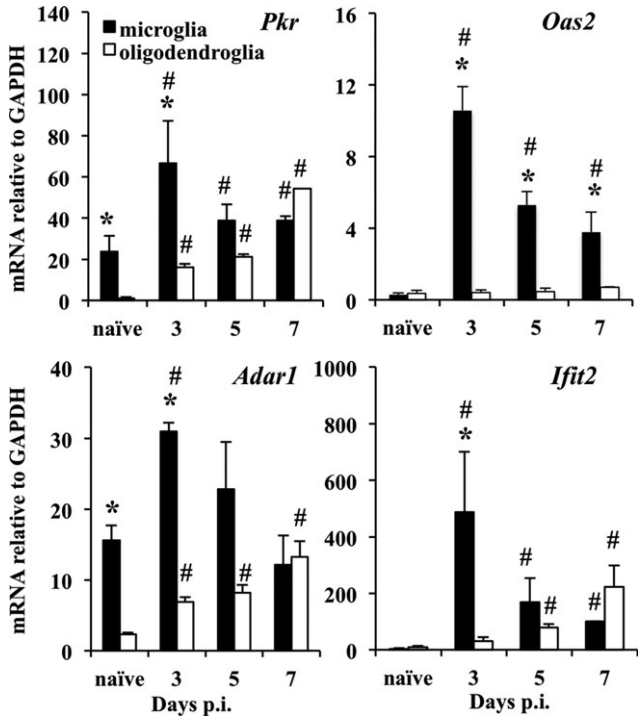

Fig. 7. Delayed induction of antiviral ISG in oligodendroglia. Microglia and oligodendroglia from naïve or JHMV infected mice were assayed for *Pkr, Oas2, Adar1*, and *Ifit2* transcripts as indicated in Fig. 1. Data represent the average of three separate experiments ± SEM. "*" denotes $P \leq 0.05$ comparing microglia to oligodendroglia at each timepoint; "#" indicates $P \leq 0.05$ compared with basal levels for each cell population.

and declined thereafter. With the exception of *Oas2*, induction was also evident at Day 3 p.i. in oligodendroglia, but increases were most prominent by Day 7 p.i.; nevertheless, they never reached the peak absolute values observed in microglia (Fig. 7). These data demonstrate that oligodendroglia not only express lower steady state levels of ISGs, but also upregulate transcription with delayed kinetics relative to microglia in response to virus infection. Furthermore, delayed ISG expression in oligodendroglia indicated a more prominent responsiveness to IFNγ than IFNα/β. Overall the data clearly suggest that oligodendroglia require paracrine IFNα/β signals to induce ISG during gliatropic coronavirus infection.

Inability of Oligodendroglia to Induce *IFN*α/β Genes is Virus Independent

To test whether oligodendroglia are intrinsically limited in IFNα/β production, or if limited IFNα/β production is specific to JHMV infection, we assessed IFNα/β and ISG induction following intracerebral injection of the PRR ligand poly I:C. Poly I:C is a strong agonist of both TLR3 and the RIG-like receptors RIG-I/MDA5 (Alexopoulou et al., 2001; Kato et al., 2006). *Ifn*α/β upregulation was initially tested in total tissue to characterize the time course of poly I:C induced IFNα/β responses in the CNS. *Ifn*β expression was maximal at 2 h and *Ifnα4* mRNA was elevated between 2 and 12 h post poly I:C inoculation (Fig. 8). By contrast, peak induction of the ISGs *Ifit1* and *Ifit2* was delayed until 12 h (Fig. 8). Cell type-specific gene analysis of IFNα/β and ISG after intracerebral poly I:C injection was thus performed in purified microglia and oligodendroglia at 4 h as an intermediate timepoint for optimal *Ifn*α/β expression and at 12 h. In microglia *Ifna4* and *Ifn*β transcripts were clearly induced by 4 h and expression of *Ifn*β was sustained until 12-h postinoculation (Fig. 9). Importantly, the 30–40 fold higher levels than those induced by viral infection (see Fig. 4), were consistent with the low viral loads in the microglia population. Importantly however, *Ifn*α/β mRNA remained near detection thresholds in oligodendroglia (Fig. 9). *Mda5* and *Rig-I* levels were also increased more robustly in both cell populations after poly I:C injection relative to virus infection (Fig. 9). Furthermore, similar to the trend observed during infection, *Rig-I* transcripts were significantly increased over *Mda5* transcripts in oligodendroglia. Nevertheless, *Ikk*ε and *Irf7* transcripts were elevated in both microglia and oligodendroglia at 4 and 12 h after poly I:C (Fig. 9) relative to viral infection (Fig. 5). While limiting IFNα/β levels thus clearly contributed to suboptimal ISG induction in both glial populations following infection, the mechanisms underlying the paucity of IFNα/β induction specifically in oligodendroglia remain elusive. Representative of antiviral ISG expression, *Ifit1* and *Ifit2* mRNA were also increased in microglia at 4 h, but subsided by 12 h post poly I:C administration. By contrast, *Ifit1* and *Ifit2* induced in oligodendroglia at 4 h were lower than in microglia, but were sustained at 12 h

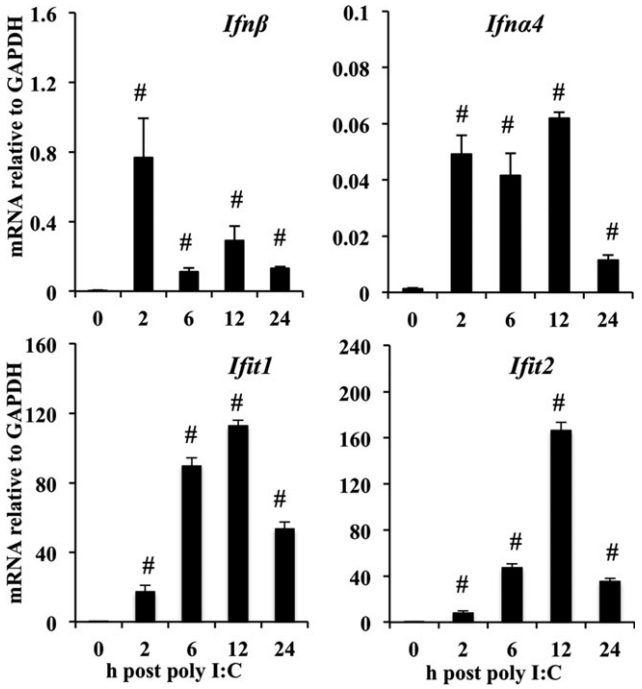

Fig. 8. Kinetics of CNS IFNα/β responses to poly I:C. Wt mice were injected intracerebrally with 200 μg poly I:C to assess kinetics of *Ifn*β, *Ifnα4, Ifit1, and Ifit2* mRNA induction in spinal cords. Data represent the mean ± SEM for three mice per group; "#" indicates $P \leq 0.05$ compared with basal levels.

(Fig. 9). Even under these conditions of infection independent *in vivo* stimulation, oligodendroglia exhibited tentative and delayed ISG induction. These results were further supported by isolating microglia and oligodendroglia from naïve adult mice and stimulating each population *ex vivo* with poly I:C in the presence of FuGENE to trigger intracellular PRR activation (Supp. Info. Fig. 2). FuGENE dramatically increased transcription of *Ifn*α/β in microglia 8 h post poly I:C stimulation. However, under similar conditions, *Ifn*α/β mRNA remained below detection in oligodendroglia. Similarly, induction of *Ifit1 and Ifit2* mRNA was increased greater than threefold in microglia treated with both poly I:C and FuGENE, compared with poly I:C alone, supporting enhanced IFNα/β mediated induction. By contrast, although *Ifit1 and Ifit2* mRNA induction was detectable in treated oligodendroglia, overall levels were significantly reduced, supporting an inherently low, if any capacity to induce *Ifn*α/β mRNA. Overall our results support the notion that *in vivo* oligodendroglia are not only intrinsically impaired in inducing IFNα/β in response to RNA stimuli, but also in responsiveness to IFNα/β suggesting an overall dampened capacity for innate responses.

DISCUSSION

PRR initiated innate responses in the CNS are critical for the induction of IFNα/β, as well proinflammatory cytokines and chemokines. While PRR expression and

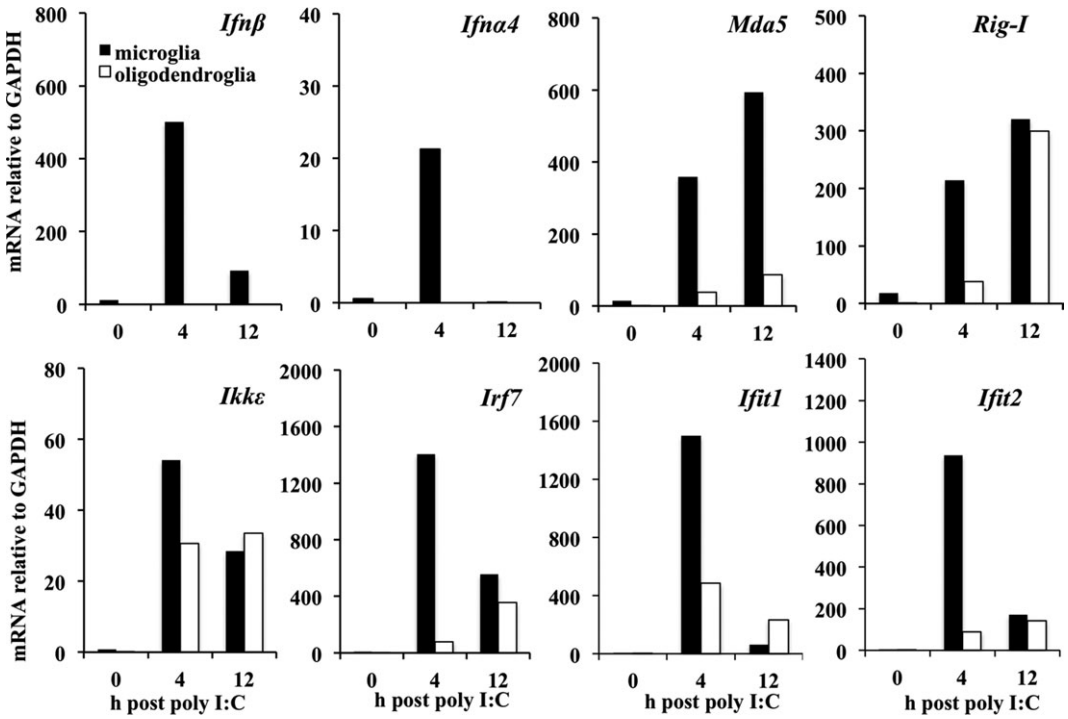

Fig. 9. Distinct *in vivo* responses of oligodendroglia and microglia to poly I:C. Microglia and oligodendroglia purified from spinal cords at 4 or 12 h post poly I:C injection were analyzed for expression of *Ifnα4, Ifnβ, Mda5, Rig-I, Ikkε*, *Irf7*, *Ifit1, and Ifit2* transcripts. Data are representative of two independent experiments each with 10 pooled mice per experiment.

activation in microglia and astrocytes has been extensively explored *in vitro* (Butchi et al., 2010; Carpentier et al., 2008; Jin et al., 2011; So and Kim, 2009), expression of PRR and associated signaling components in glia *in vivo* are poorly defined, especially in oligodendroglia. In this study we compared the capacity of oligodendroglia relative to microglia to mount IFNα/β mediated innate immune responses. Glial specific responses were monitored within the context of the CNS following intracerebral infection of adult mice with gliatropic JHMV or injection of poly I:C. Microglia were prominent inducers of *Ifn*α/β mRNA following infection, consistent with IFNα/β induction in primary microglia as well as bone marrow derived macrophages infected with a heterologous MHV (Roth-Cross et al., 2008). However, the inability of oligodendroglia to induce *Ifn*α/β mRNA, despite their high load of viral RNA, contrasted with *in vitro* studies demonstrating MDA5 and RIG-I dependent IFNα/β induction in the infected N20.1 oligodendroglia cell line (Li et al., 2010). This discrepancy likely reflects differences in expression and/or induction of IFNα/β pathway components, rather than distinct viral loads, as even poly I:C did not induce *Ifn*α/β in oligodendroglia *in vivo* or *ex vivo*.

The restricted ability of coronaviruses to induce IFNα/β was recently attributed to the O-methylated cap structure of the viral RNA, making it difficult for the host to distinguish viral from self mRNA (Daffis et al., 2010; Zust et al., 2011). However, in contrast to cultured fibroblasts, bone marrow-derived dendritic cells, astrocytes, and neurons, the ability of plasmacytoid dendritic cells, macrophages/microglia, and an oligodendroglia cell line to induce IFNα/β via TLR7, MDA5 and MDA5/RIG-I dependent pathways (Cervantes-Barragan et al., 2007; Li et al., 2010; Roth-Cross et al., 2008; Zhou and Perlman, 2007) suggests sufficient PRR activation by viral RNA structures to mediate protective responses in select cell types. Our data indicate that cell type-specific basal expression, as well as inducible components in the innate signaling pathway constitute critical signaling thresholds determining IFNα/β induction. In the adult CNS oligodendroglia differed significantly from microglia in reduced basal transcript levels of viral RNA sensing PRRs and *Ikkε*. However, basal *Irf3* transcripts were only reduced by ~50%, and *Irf7* transcripts were barely detectable in either cell population, consistent with higher basal *Irf3* than *Irf7* levels observed in whole naïve brains (Ousman et al., 2005). Reduced basal PRR levels in oligodendroglia were reminiscent of sparsely expressed PRRs in primary neurons (Carpentier et al., 2008), and supported the superior initiation of *Ifn*α/β responses by microglia. This concept is consistent with the inability of primary cultured neurons and astrocytes to induce IFNα/β expression following MHV infection (Roth-Cross et al., 2008). It remains to be confirmed whether other CNS infections involving oligodendroglia reveal a similarly muted pattern of IFNα/β induction and responsiveness. However, most RNA viruses are

neuronotropic, with only some variants of Theilers murine encephalomyelitis virus displaying tropism for oligodendroglia in mouse strains susceptible to persistent infection (Brahic et al., 2005). However, during the acute CNS infection, this virus primarily infects neurons and oligodendroglia and is only infected during the persistent stage, making direct comparisons difficult.

Optimal IFNα/β induction requires amplification through IFNAR to elevate PRRs and IRF7 (Honda and Taniguchi, 2006; Honda et al., 2005; Malmgaard et al., 2002). However, in contrast to *Ifn*α/β induction, IFNAR signaling was intact in oligodendroglia. Although IFNα/β protein was below detection in cell-free supernatants derived from the JHMV infected CNS by ELISA (data not shown), IFNα/β sufficed to upregulate the ISGs *Mda5*, *Rig-I*, *Stat1*, *Irf7*, *Pkr*, *Ifit2*, and *Adar1* in oligodendroglia. The ability of IFNα/β to induce ISGs was consistent with basal expression of IFNAR chains, as well as basal and inducible levels of *Stat1* and *Irf9* transcripts. Although induction above basal levels was greater in oligodendroglia than microglia for some genes, peak absolute mRNA levels were in general lower compared with those reached in microglia, as exemplified by *Stat1* and *Irf7* mRNA. Furthermore, peak expression for many genes did not correlate with maximal *Ifn*α/β mRNA levels, but rather with peak IFNγ mRNA and protein at Day 7 p.i. (Phares et al., 2011). The distinct pattern of ISG expression in oligodendroglia compared with microglia may further reside in low IKKε. In addition to mediating PRR signaling, IKKε influences ISG induction through participation in JAK/STAT mediated IFNα/β signaling (Pham and Tenoever, 2010; Tenoever et al., 2007). Although not as severe as the complete abrogation of ISG induction in STAT1$^{-/-}$ mice, IKKε$^{-/-}$ mice lack induction of ~30% of ISGs, including *Adar1* (Durbin et al., 1996; Tenoever et al., 2007). The biological consequences are demonstrated by impaired clearance of influenza virus infection by IKKε$^{-/-}$ mice, despite similar expression of IL2, IL6, IL12, IFNγ, and RANTES as well as induction of antiviral antibody (Tenoever et al., 2007). The paucity of *Ikk*ε mRNA and modest, if any, increase of *Irf7* mRNA in oligodendroglia, despite abundant viral and *Mda5* mRNA upregulation, may partially explain the absence of *Ifn*α/β expression and more selective and delayed ISG induction during infection. However, even the strong IFNα/β response elicited in microglia by poly I:C did not overcome the inability of oligodendroglia to induce *Ifn*α/β, despite the overall higher increases in *Ikk*ε and *Irf7* transcripts relative to those induced by infection. These results suggest additional restrictions intrinsic to oligodendroglia in the initiation of IFNα/β production. Furthermore, limited ISG expression by oligodendroglia following infection can partially be attributed to overall low IFNα/β induction by JHMV, as upregulation of the prominently IFNα/β dependent *Ifit1* and *Ifit2* mRNAs was enhanced in both microglia and oligodendroglia following poly I:C administration relative to infection. These results suggest that the ability of oligodendroglia to respond to IFNα/β is dependent on the overall availability of IFNα/β in the local environment.

The results thus indicate a reliance of oligodendroglia on external production of IFNα/β to induce an antiviral state. This concept is consistent with data indicating that microglia are a dominant source of IFNα/β within the CNS during JHMV induced encephalomyelitis (Roth-Cross et al., 2008). The biological relevance of suboptimal IFNα/β responses is clearly evident from differential viral control in both cell types. A direct response to infection by microglia is supported by the correlation between peak viral and *Ifn*α/β mRNA. Furthermore, the early decline in viral RNA, prior to infiltration of T cells, indicates autocrine IFNα/β contributes to the rapid control of virus in this cell type. By contrast, although oligodendroglia were initially infected to a lesser extent than microglia, viral RNA increased over 2 logs between Days 3 and 5 p.i., coincident with no *Ifn*α/β and tentative induction of antiviral ISGs. These data indicate that oligodendroglia rely largely on T cell effector function, prominently IFNγ, for viral control (Parra et al., 2010). Oligodendroglia are indeed highly responsive to IFNγ as indicated by upregulation of Class I MHC molecules and associated antigen processing components during peak IFNγ, but not IFNα/β induction during JHMV infection (Malone et al., 2008). Moreover, specific blockade of IFNγ receptor signaling on oligodendroglia prolongs JHMV infection in this cell type (Gonzalez et al., 2005, 2006; Parra et al., 2010). Whether early events favoring robust infection of oligodendroglia prior to emergence of T cells, contribute to ultimate persistence of JHMV in oligodendroglia, remains to be elucidated.

Overall our results demonstrate a limited role of oligodendroglia as both inducers of, and responders to, IFNα/β compared with microglia. Limited innate antiviral activity may predispose oligodendroglia to be potent responders to IFNγ (Gonzalez et al., 2005; Popko and Baerwald, 1999). While there is no evidence supporting toxicity of IFNα/β (Akwa et al., 1998), more restricted induction of antiviral mediators, especially those also affecting host cell translation, may circumvent apoptosis and guarantee maintenance of critical myelin housekeeping functions and survival. Our findings also contradict the hypothesis suggesting that virus initiated IFNα/β production by oligodendroglia drives inflammatory responses during viral-induced demyelinating disease (Lipton et al., 2007). The low abundance of PRR at basal levels rather provide a mechanism underlying the apparent paucity of oligodendroglia to express cytokines during multiple sclerosis or other CNS inflammatory conditions (Cannella and Raine, 2004; Zeis et al., 2008). Our data thus support the notion that oligodendroglia are defensive players under inflammatory conditions.

ACKNOWLEDGMENTS

The authors thank Ms. Jennifer Powers for cell sorting, Dr. Timothy W. Phares for breeding PLP-GFP mice, and Dr. Joan Durbin (New York University Langone Medical Center) for providing primer sequences for IFNλ.

REFERENCES

Akwa Y, Hassett DE, Eloranta ML, Sandberg K, Masliah E, Powell H, Whitton JL, Bloom FE, Campbell IL. 1998. Transgenic expression of IFN-alpha in the central nervous system of mice protects against lethal neurotropic viral infection but induces inflammation and neurodegeneration. J Immunol 161:5016–5026.

Alexopoulou L, Holt AC, Medzhitov R, Flavell RA. 2001. Recognition of double-stranded RNA and activation of NF-kappaB by Toll-like receptor 3. Nature 413:732–738.

Barton GM. 2008. A calculated response: Control of inflammation by the innate immune system. J Clin Invest 118:413–420.

Bass BL. 1997. RNA editing and hypermutation by adenosine deamination. Trends Biochem Sci 22:157–162.

Bergmann CC, Lane TE, Stohlman SA. 2006. Coronavirus infection of the central nervous system: Host-virus stand-off. Nat Rev Microbiol 4:121–132.

Borden EC, Sen GC, Uze G, Silverman RH, Ransohoff RM, Foster GR, Stark GR. 2007. Interferons at age 50: Past, current, and future impact on biomedicine. Nat Rev Drug Discov 6:975–990.

Brahic M, Bureau JF, Michiels T. 2005. The genetics of the persistent infection and demyelinating disease caused by Theiler's virus. Annu Rev Microbiol 59:279–298.

Bsibsi M, Ravid R, Gveric D, van Noort JM. 2002. Broad expression of Toll-like receptors in the human central nervous system. J Neuropathol Exp Neurol 61:1013–1021.

Butchi NB, Du M, Peterson KE. 2010. Interactions between TLR7 and TLR9 agonists and receptors regulate innate immune responses by astrocytes and microglia. Glia 58:650–664.

Cannella B, Raine CS. 2004. Multiple sclerosis: Cytokine receptors on oligodendrocytes predict innate regulation. Ann Neurol 55:46–57.

Carpentier PA, Duncan DS, Miller SD. 2008. Glial toll-like receptor signaling in central nervous system infection and autoimmunity. Brain Behav Immun 22:140–147.

Carty M, Bowie AG. 2011. Evaluating the role of Toll-like receptors in diseases of the central nervous system. Biochem Pharmacol 81:825–837.

Cervantes-Barragan L, Zust R, Weber F, Spiegel M, Lang KS, Akira S, Thiel V, Ludewig B. 2007. Control of coronavirus infection through plasmacytoid dendritic-cell-derived type I interferon. Blood 109:1131–1137.

Colonna M. 2007. TLR pathways and IFN-regulatory factors: To each its own. Eur J Immunol 37:306–309.

Daffis S, Szretter KJ, Schriewer J, Li J, Youn S, Errett J, Lin TY, Schneller S, Zust R, Dong H, Thiel V, Sen GC, Fensterl V, Klimstra WB, Pierson TC, Buller RM, Gale M Jr, Shi PY, Diamond MS. 2010. 2′-O methylation of the viral mRNA cap evades host restriction by IFIT family members. Nature 468:452–456.

Delhaye S, Paul S, Blakqori G, Minet M, Weber F, Staeheli P, Michiels T. 2006. Neurons produce type I interferon during viral encephalitis. Proc Natl Acad Sci USA 103:7835–7840.

Domanski P, Witte M, Kellum M, Rubinstein M, Hackett R, Pitha P, Colamonici OR. 1995. Cloning and expression of a long form of the beta subunit of the interferon alpha beta receptor that is required for signaling. J Biol Chem 270:21606–21611.

Dong Y, Benveniste EN. 2001. Immune function of astrocytes. Glia 36:180–190.

Durbin JE, Hackenmiller R, Simon MC, Levy DE. 1996. Targeted disruption of the mouse Stat1 gene results in compromised innate immunity to viral disease. Cell 84:443–450.

Fleming JO, Trousdale MD, el-Zaatari FA, Stohlman SA, Weiner LP. 1986. Pathogenicity of antigenic variants of murine coronavirus JHM selected with monoclonal antibodies. J Virol 58:869–875.

Fuss B, Mallon B, Phan T, Ohlemeyer C, Kirchhoff F, Nishiyama A, Macklin WB. 2000. Purification and analysis of in vivo-differentiated oligodendrocytes expressing the green fluorescent protein. Dev Biol 218:259–274.

Gonzalez JM, Bergmann CC, Fuss B, Hinton DR, Kangas C, Macklin WB, Stohlman SA. 2005. Expression of a dominant negative IFN-gammareceptor on mouse oligodendrocytes. Glia 51:22–34.

Gonzalez JM, Bergmann CC, Ramakrishna C, Hinton DR, Atkinson R, Hoskin J, Macklin WB, Stohlman SA. 2006. Inhibition of interferon-gamma signaling in oligodendroglia delays coronavirus clearance without altering demyelination. Am J Pathol 168:796–804.

Hanisch UK. 2002. Microglia as a source and target of cytokines. Glia 40:140–155.

Hanke ML, Kielian T. 2011. Toll-like receptors in health and disease in the brain: Mechanisms and therapeutic potential. Clin Sci (Lond) 121:367–387.

Honda K, Taniguchi T. 2006. IRFs: Master regulators of signalling by Toll-like receptors and cytosolic pattern-recognition receptors. Nat Rev Immunol 6:644–658.

Honda K, Yanai H, Negishi H, Asagiri M, Sato M, Mizutani T, Shimada N, Ohba Y, Takaoka A, Yoshida N, et al. 2005. IRF-7 is the master regulator of type-I interferon-dependent immune responses. Nature 434:772–777.

Ireland DD, Stohlman SA, Hinton DR, Atkinson R, Bergmann CC. 2008. Type I interferons are essential in controlling neurotropic coronavirus infection irrespective of functional CD8 T cells. J Virol 82:300–310.

Ireland DD, Stohlman SA, Hinton DR, Kapil P, Silverman RH, Atkinson RA, Bergmann CC. 2009. RNase L mediated protection from virus induced demyelination. PLoS Pathog 5:e1000602.

Jin YH, Kim SJ, So EY, Meng L, Colonna M, Kim BS. 2011. Melanoma differentiation-associated gene 5 is critical for protection against Theiler's virus-induced demyelinating disease. J Virol 86:1531–1543.

Kapil P, Atkinson R, Ramakrishna C, Cua DJ, Bergmann CC, Stohlman SA. 2009. Interleukin-12 (IL-12), but not IL-23, deficiency ameliorates viral encephalitis without affecting viral control. J Virol 83:5978–5986.

Kato H, Takeuchi O, Sato S, Yoneyama M, Yamamoto M, Matsui K, Uematsu S, Jung A, Kawai T, Ishii KJ, et al. 2006. Differential roles of MDA5 and RIG-I helicases in the recognition of RNA viruses. Nature 441:101–105.

Kawai T, Akira S. 2007. Antiviral signaling through pattern recognition receptors. J Biochem 141:137–145.

Kawai T, Akira S. 2009. The roles of TLRs, RLRs and NLRs in pathogen recognition. Int Immunol 21:317–337.

Levy DE, Garcia-Sastre A. 2001. The virus battles: IFN induction of the antiviral state and mechanisms of viral evasion. Cytokine Growth Factor Rev 12:143–156.

Li J, Liu Y, Zhang X. 2010. Murine coronavirus induces type I interferon in oligodendrocytes through recognition by RIG-I and MDA5. J Virol 84:6472–6482.

Lipton HL, Liang Z, Hertzler S, Son KN. 2007. A specific viral cause of multiple sclerosis: One virus, one disease. Ann Neurol 61:514–523.

Malmgaard L, Salazar-Mather TP, Lewis CA, Biron CA. 2002. Promotion of alpha/beta interferon induction during in vivo viral infection through alpha/beta interferon receptor/STAT1 system-dependent and -independent pathways. J Virol 76:4520–4525.

Malone KE, Stohlman SA, Ramakrishna C, Macklin W, Bergmann CC. 2008. Induction of class I antigen processing components in oligodendroglia and microglia during viral encephalomyelitis. Glia 56:426–435.

McKimmie CS, Johnson N, Fooks AR, Fazakerley JK. 2005. Viruses selectively upregulate Toll-like receptors in the central nervous system. Biochem Biophys Res Commun 336:925–933.

Mogensen TH. 2009. Pathogen recognition and inflammatory signaling in innate immune defenses. Clin Microbiol Rev 22:240–273 (Table of Contents).

Okun E, Griffioen KJ, Lathia JD, Tang SC, Mattson MP, Arumugam TV. 2009. Toll-like receptors in neurodegeneration. Brain Res Rev 59:278–292.

Ousman SS, Wang J, Campbell IL. 2005. Differential regulation of interferon regulatory factor (IRF)-7 and IRF-9 gene expression in the central nervous system during viral infection. J Virol 79:7514–7527.

Parra GI, Bergmann CC, Phares TW, Hinton DR, Atkinson R, Stohlman SA. 2010. Gamma interferon signaling in oligodendrocytes is critical for protection from neurotropic coronavirus infection. J Virol 84:3111–3115.

Paul S, Ricour C, Sommereyns C, Sorgeloos F, Michiels T. 2007. Type I interferon response in the central nervous system. Biochimie 89:770–778.

Pham AM, Tenoever BR. 2010. The IKK kinases: Operators of antiviral signaling. Viruses 2:55–72.

Phares TW, Marques CP, Stohlman SA, Hinton DR, Bergmann CC. 2011. Factors supporting intrathecal humoral responses following viral encephalomyelitis. J Virol 85:2589–2598.

Phares TW, Ramakrishna C, Parra GI, Epstein A, Chen L, Atkinson R, Stohlman SA, Bergmann CC. 2009. Target-dependent B7-H1 regulation contributes to clearance of central nervous system infection and dampens morbidity. J Immunol 182:5430–5438.

Popko B, Baerwald KD. 1999. Oligodendroglial response to the immune cytokine interferon gamma. Neurochem Res 24:331–338.

Roth-Cross JK, Bender SJ, Weiss SR. 2008. Murine coronavirus mouse hepatitis virus is recognized by MDA5 and induces type I interferon in brain macrophages/microglia. J Virol 82:9829–9838.

Sen GC. 2001. Viruses and interferons. Annu Rev Microbiol 55:255–281.

Serafini B, Columba-Cabezas S, Di Rosa F, Aloisi F. 2000. Intracerebral recruitment and maturation of dendritic cells in the onset and progression of experimental autoimmune encephalomyelitis. Am J Pathol 157:1991–2002.

Sharma A, Maheshwari RK. 2009. Oligonucleotide array analysis of Toll-like receptors and associated signalling genes in Venezuelan equine encephalitis virus-infected mouse brain. J Gen Virol 90(Part 8):1836–1847.

Shrestha B, Gottlieb D, Diamond MS. 2003. Infection and injury of neurons by West Nile encephalitis virus. J Virol 77:13203–13213.

Skinner MA, Siddell SG. 1983. Coronavirus JHM: Nucleotide sequence of the mRNA that encodes nucleocapsid protein. Nucleic Acids Res 11:5045–5054.

So EY, Kim BS. 2009. Theiler's virus infection induces TLR3-dependent upregulation of TLR2 critical for proinflammatory cytokine production. Glia 57:1216–1226.

Sommereyns C, Paul S, Staeheli P, Michiels T. 2008. IFN-lambda (IFN-lambda) is expressed in a tissue-dependent fashion and primarily acts on epithelial cells in vivo. PLoS Pathogens 4:e1000017.

Stetson DB, Medzhitov R. 2006. Type I interferons in host defense. Immunity 25:373–381.

Stewart MJ, Smoak K, Blum MA, Sherry B. 2005. Basal and reovirus-induced beta interferon (IFN-beta) and IFN-beta-stimulated gene expression are cell type specific in the cardiac protective response. J Virol 79:2979–2987.

Tenoever BR, Ng SL, Chua MA, McWhirter SM, Garcia-Sastre A, Maniatis T. 2007. Multiple functions of the IKK-related kinase IKKepsilon in interferon-mediated antiviral immunity. Science 315:1274–1278.

van Noort JM, Bsibsi M. 2009. Toll-like receptors in the CNS: Implications for neurodegeneration and repair. Prog Brain Res 175:139–148.

Vilcek J. 2006. Fifty years of interferon research: Aiming at a moving target. Immunity 25:343–348.

Zeis T, Graumann U, Reynolds R, Schaeren-Wiemers N. 2008. Normal-appearing white matter in multiple sclerosis is in a subtle balance between inflammation and neuroprotection. Brain 131(Part 1):288–303.

Zhou H, Perlman S. 2007. Mouse hepatitis virus does not induce Beta interferon synthesis and does not inhibit its induction by double-stranded RNA. J Virol 81:568–574.

Zust R, Cervantes-Barragan L, Habjan M, Maier R, Neuman BW, Ziebuhr J, Szretter KJ, Baker SC, Barchet W, Diamond MS, et al. 2011. Ribose 2′-O-methylation provides a molecular signature for the distinction of self and non-self mRNA dependent on the RNA sensor Mda5. Nat Immunol 12:137–143.